Virginia Commonwealth University
VCU Scholars Compass

Theses and Dissertations | Graduate School

2022

Periodic Trends in the Infrared and Optical Absorption Spectra of Metal Chalcogenide Clusters

Alain Ward
Virginia Commonwealth University

Follow this and additional works at: https://scholarscompass.vcu.edu/etd

Part of the Atomic, Molecular and Optical Physics Commons, and the Condensed Matter Physics Commons

© The Author

Downloaded from
https://scholarscompass.vcu.edu/etd/7032

This Thesis is brought to you for free and open access by the Graduate School at VCU Scholars Compass. It has been accepted for inclusion in Theses and Dissertations by an authorized administrator of VCU Scholars Compass. For more information, please contact libcompass@vcu.edu.

Periodic Trends in the Infrared and Optical Absorption Spectra of Metal Chalcogenide Clusters

A thesis submitted in partial fulfillment of the requirements for the degree of Master of Science at Virginia Commonwealth University

by

Alain Frederick Micah Ward

Director: Dr. Shiv N. Khanna
Commonwealth Professor
Department of Physics

Virginia Commonwealth University
Richmond, VA
May 2022

Acknowledgments

Thank you to Dr. Shiv Khanna for your guidance, wisdom, and the opportunity to work in your lab. Thank you to Dr. Arthur Reber for all of your guidance, help, and support in this research. Thank you to Dr. Marilyn Bishop and Dr. John McMullen for teaching me the skills I needed to perform this research. Thank you to Dr. Richard Joh for teaching me computational techniques, and to Dr. Dexian Ye for teaching me experimental techniques. Thank you to Dr. Shiv Khanna, Dr. Arthur Reber, and Dr. Jayasimha Atulasimha for serving on my committee. Thank you to Ryan, Turbasu, Matthew, and Thomas for your help and support. Thank you as well to my family for your encouragement and support.

Table of Contents

List of Abbreviations iv

ABSTRACT v

I. Introduction 1

1.1 Background 1

1.2 Motivation 10

II. Methods 13

2.1 DFT 13

2.2 ADF 15

III. Results and Discussion 17

3.1 Structure of Clusters 17

3.2 Optical Spectroscopy in TMCC's 19

3.3 Energetics Results 22

3.4 Infrared Frequency Results 24

IV. Conclusions 33

V. Bibliography 35

List of Abbreviations

ADF:	Amsterdam Density Functional
IR:	Infrared Spectroscopy
OP:	Optical Spectroscopy
MC:	Metal Chalcogenide
TMCC:	Transition Metal Chalcogenide Clusters
DFT:	Density Functional Theory
TD-DFT:	Time Dependent Density Functional Theory
XC:	Exchange–Correlation
SCF:	Self Consistent Field
LES:	Lowest Excitation State

ABSTRACT

We have investigated the Optical absorption, Infrared spectra, Binding Energies, and various other cluster properties to determine the existence of periodic trend for Transition Metal Chalcogenide Clusters ligated with CO ligands. We were motivated by the prospect of answering the question whether periodic behavior can be observed in properties of octahedral metal-chalcogenide clusters. To answer this question, we have used the Amsterdam Density Functional code to calculate the electronic structure of Transition Metal Chalcogenide Clusters using gradient-corrected density functional theory. During the course of our investigation, we determined the existence of several periodic trends in properties of octahedral Transition Metal Chalcogenide Clusters $TM_6Se_8(CO)_6$. In order to investigate these trends, the ground state, optical spectra, and infrared spectra of ligated transition metal chalcogenide clusters with valence electron counts ranging from 90-116 were calculated. We found that octahedral metal-chalcogenide clusters with 96, 100, and 114 have larger excitation energies, consistent with these clusters having closed-electronic shells and longer gap between the highest occupied and lowest unoccupied orbitals. Periodic trends were also observed in the Infrared spectra, with the CO bond stretch having the highest energy at 100 and 114 valence electrons due to the closed-electronic shell minimizing back-bonding with the CO molecule. A periodic trend in the antisymmetric TM-C stretch was also observed, with the vibrational energy increasing as the valence electron count increased. This is due to decrease in the TM-C bond length resulting in a larger force constant. These results reveal that periodic trends can be found in clusters other than simple or noble metal clusters, they can also be observed in symmetric transition-metal chalcogenide clusters. Further, these trends can be observed via optical and infrared spectroscopy showing that the superatom concept in metal chalcogenide clusters goes beyond electronic excitations, and can be seen in other observable properties.

I. Introduction

1.1 Background

Materials are critical to all aspects of human life. They can be found in applications ranging from textiles and clothing to building materials, food processing, vehicles, and machinery. Modern cluster research has focused on identifying new physical properties of clusters, and new theoretical frameworks to understand the notable effects that removing atoms has on those physical properties and cluster geometry. The materials used in everyday life are constructed from clusters that reside in the nanoscale size regime. In particular, clusters are of particular interests due to their strongly size-dependent properties[1]. The potential of understanding material behavior at the nanoscale has been a source of inspiration for studying nanoclusters. Nanoclusters are defined as a grouping of atoms that range in size from two to a few hundred, and inhabit the subnanoscale to nanometer size range, and are characterized by non-integer bonding. A picture of the length scale of cluster aggregates is seen in Figure 1, which can be compared to the length scales of neighboring regions. The field of nanoscale cluster science is drawing increasing attention due to the strong size and composition-dependent properties of clusters, and the exciting prospect of nanoclusters serving as the building blocks for materials with tailored properties[2]. There are many kinds of nanocluster combinations that can be created using the elements of the periodic table such as Transition Metals, which are typically malleable, ductile, and good conductors of electricity. In clusters, properties change non-monotonically and depend on Quantum Confinement, Geometric Shell Filling, and Spin effects compared to larger particles that depend on, surface/volume ratios which are variables that lead to more gradual changes. The behavior of physical properties as they depend on the number of atoms is presented in Figure 2. The behavior of physical properties is an area of important research due to the potential applications of tunable devices that can be manipulated on

the nanoscale[3]. The nanoclusters that are the focus of this paper are a class of Metal Chalcogenide clusters called Transition Metal Chalcogenide clusters.

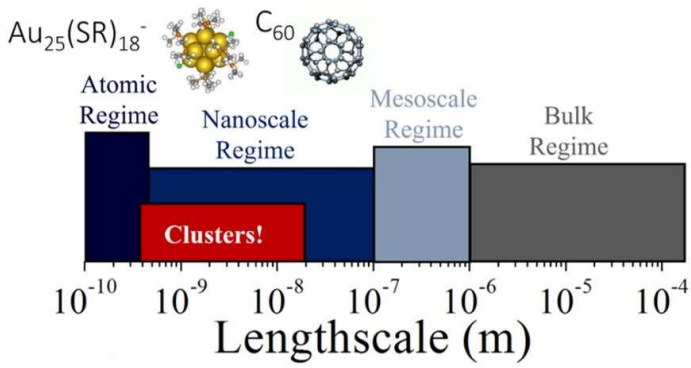

Figure 1: The Lengthscale of nanoclusters

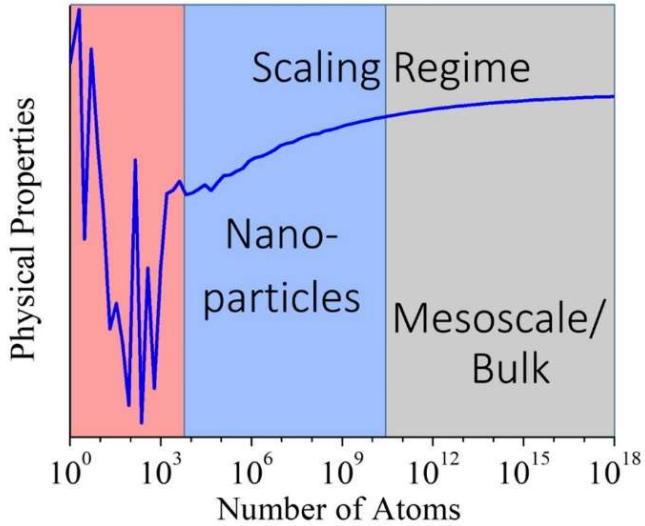

Figure 2: The dependency of Physical Properties on the number of atoms

Transition Metal chalcogenide clusters are an inorganic chemical compound group consisting of at least one chalcogen atom (S, Se, Te) and one more electropositive transition metal element.[4] Transition Metals bond strongly with chalcogens, leading to these clusters being highly stable due to covalent interaction. The location of Chalcogens on the periodic table is presented in Figure 3. For this work, we investigated if periodic properties are found in the infrared and optical frequencies of Transition Metal chalcogenides clusters. To do this, we reviewed prior literature concerning the electronic structure of various clusters, and various properties such as the binding energy, in order to determine what experiments have previously been conducted, and what results were produced. For example, the electronic structure of metal chalcogenide structures as a function of valence electrons was previously studied by the Khanna Group. They determined that the substitution of ligands within a cluster strongly affects some of the electronic properties of the cluster [5]. In addition, the effect of chalcogen and metal on the electronic properties and stability of metal-chalcogenide clusters has been well documented for a variety of clusters [6]. The Khanna Group wanted to analyze the electronic structure of metal–chalcogen clusters and identify if these clusters have periodic closed electronic shells that can lead to superatomic states with a well-defined valence. The key criterion for a cluster to be considered a superatom is that the cluster has a well-defined valence. For the valence to be identified, the Khanna Group had to find valence electron counts that correspond to enhanced stability. More research concerning the properties of large clusters has been conducted by the Roy Group, led by Xavier Roy. The Roy Group has utilized Superatoms, such as $Cr_6Se_8(PR_3)_6$, $Co_6Te_8(PR_3)_6$, and $Ni_9Te_6(PR_3)_8$ as seen in Figure 6.[7] In particular, the Roy Group has used Re_6Se_8, in the process of synthesizing surface-functionalized 2D superatomic materials due to its stability properties: $Re_6Se_8I_2$, $Re_6Se_8(SPh)_2$, $Re_6Se_8(SPhNH_2)_2$, and $Re_6Se_8(SC_{16}H_{33})_2$, with chemically modified surfaces and properties.[7] Also, the

Roy Group has studied the cluster assembly of Superatoms as a means to assemble stable 2D materials. Due to these results and similar conclusions, we wanted to understand if TMCC are stable can they be considered Superatoms. Pictures of some of the potential applications of Metal Chalcogenides are presented in Figures 4 and 5.

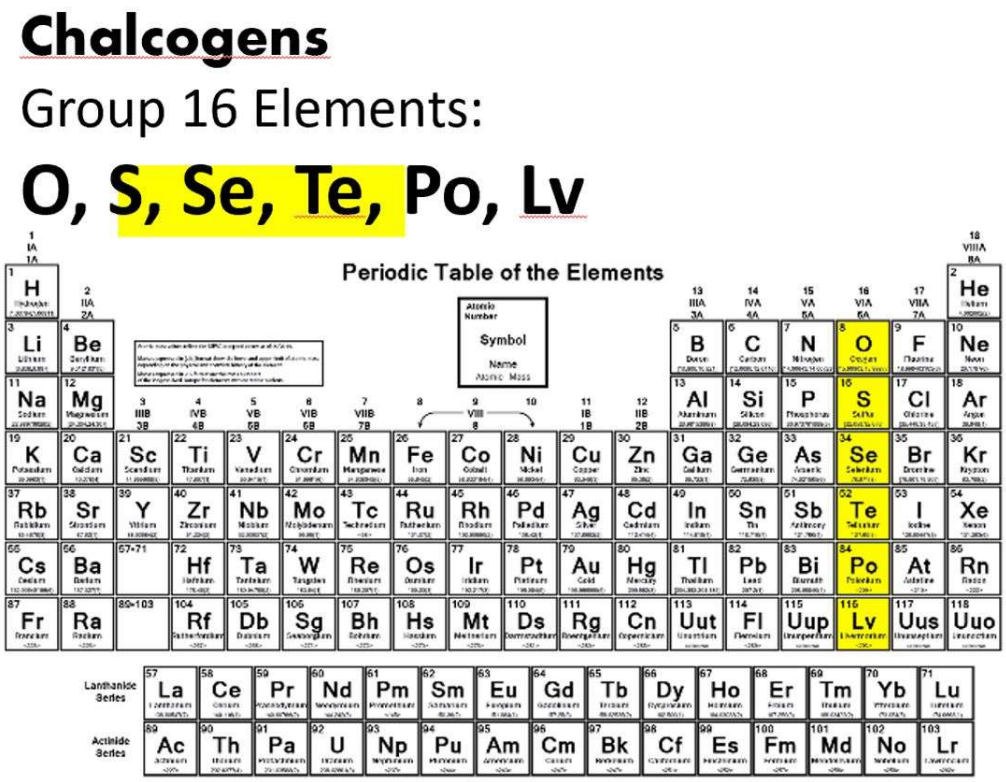

Figure 3: The location of Chalcogens on the periodic table

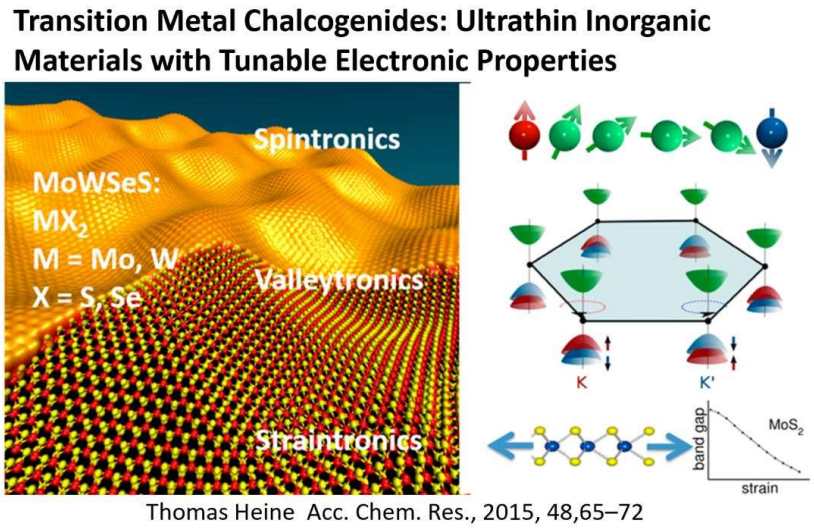

Figure 4: Potential applications of TMCC with tunable properties

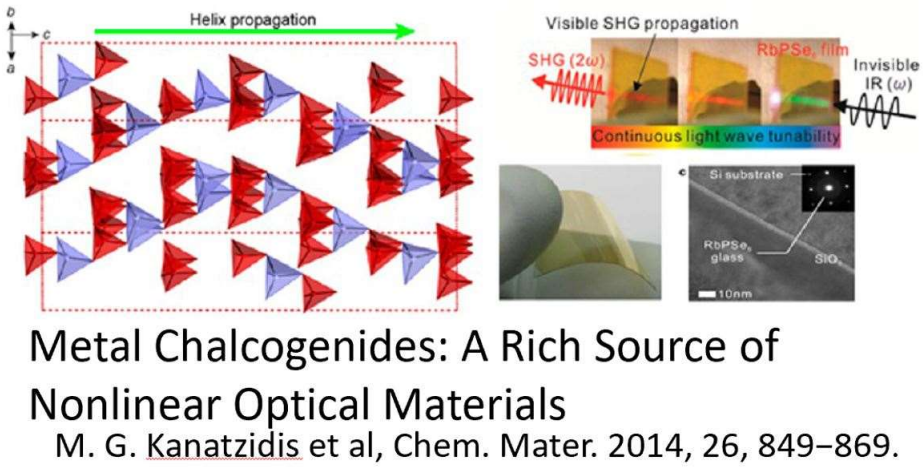

Figure 5: Potential of TMCC to be used as Nonlinear Optical Materials

As previously mentioned, the Khanna Group's, and many other research groups, investigations into the electronic structure of metal chalcogenide clusters are built on the concept of a Superatom structure, which is any cluster of atoms that seem to exhibit some of the properties of elemental atoms. The reason for this is that the clusters have a well-defined valence due to an electronic shell closing. A figure displaying examples of Metal Chalcogenide Superatoms is seen in Figure 6. Because of the unique characteristics of Superatoms and their commercial potential, Superatoms have drawn increasing attention from research groups due to their potential to act as building blocks for novel cluster materials with variable properties, and this interest has led to numerous collaborative research efforts, such as the experimental Superatom work carried out by the Roy Research Group, in collaboration with the Khanna Group. The Roy Group determined that Superatom materials show great promise for use in a versatile approach to create 2D materials with tunable physical and chemical properties depending on the chemistry of the 2D region [8]. Finally, research by the Roy Group has investigated the electronic structure of Superatoms, and their stability compared to the stability of single atoms. The different types of stabilization seen in Superatom structures are presented in Figure 8. Results from prior literature show that the electronic structure of atoms is different from the electronic structure of clusters, which is presented in Figure 7. However, the enhanced electronic stability possessed by atoms and Superatoms, with filled shells, displays the ability of Superatoms to demonstrate characteristics of single atoms [9]. Additional research has also been conducted into the change of electronic structure of thin films, as the band gap is altered by geometric confinement [10]. The Khanna Group has also studied the effect of ligands acting on aluminum-iodine clusters, which showed that ligands can alter the electronic structure of clusters and enhance the stability [11]. In addition, pictures of ligand

protected Superatom structures are presented in Figure 9 to display Superatom structures with ligands.

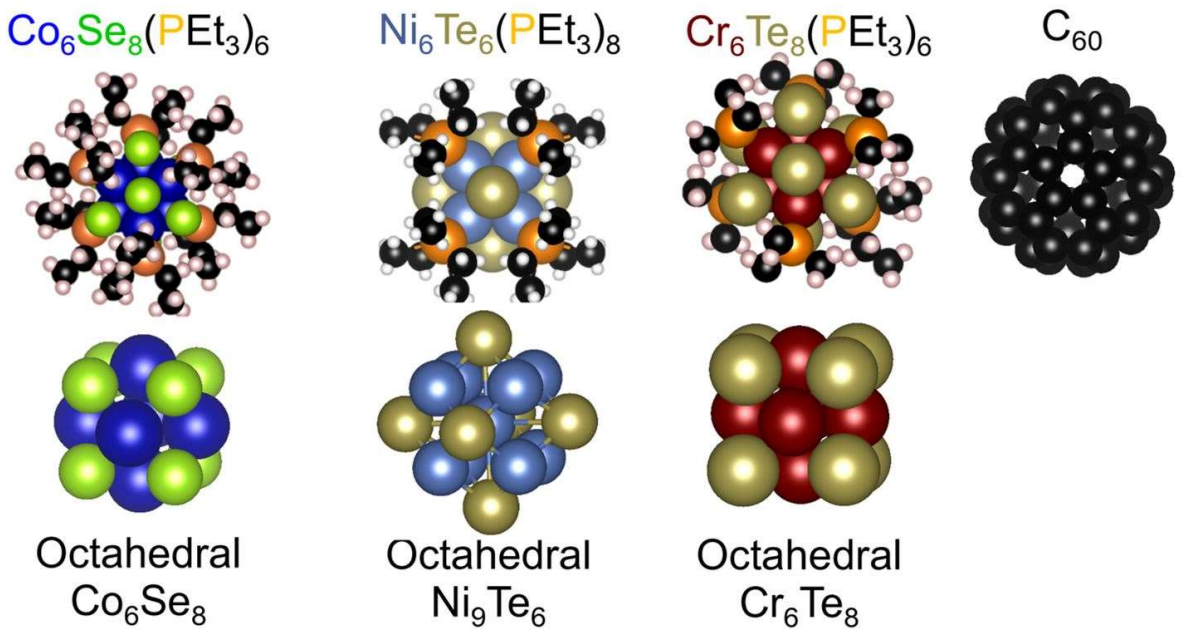

Figure 6: Examples of Metal Chalcogenide Superatoms

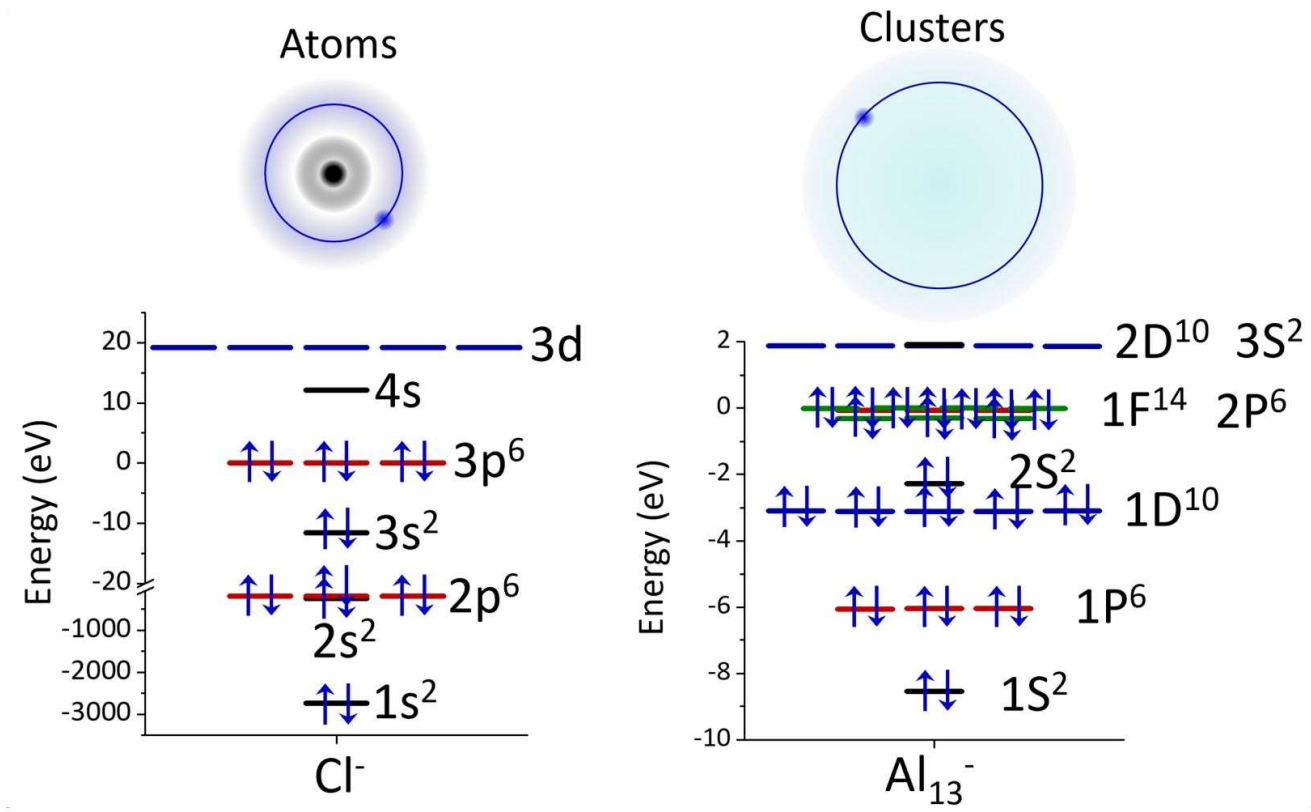

Figure 7: Electronic Structure of Atoms vs Clusters

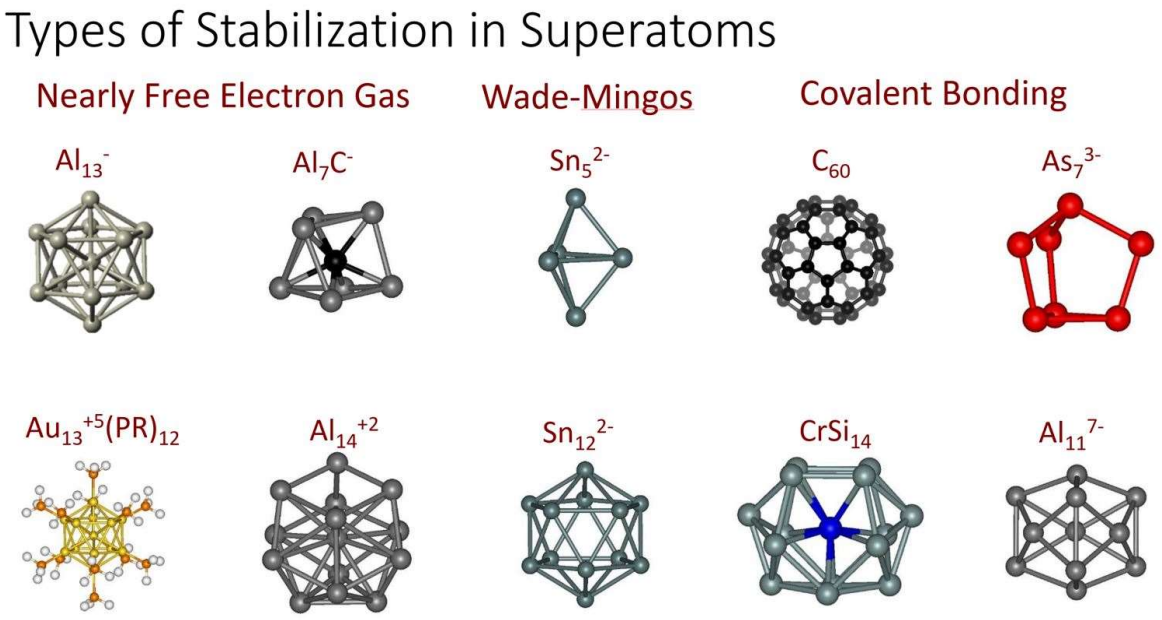

Figure 8: Examples of the types of stabilization in Superatoms

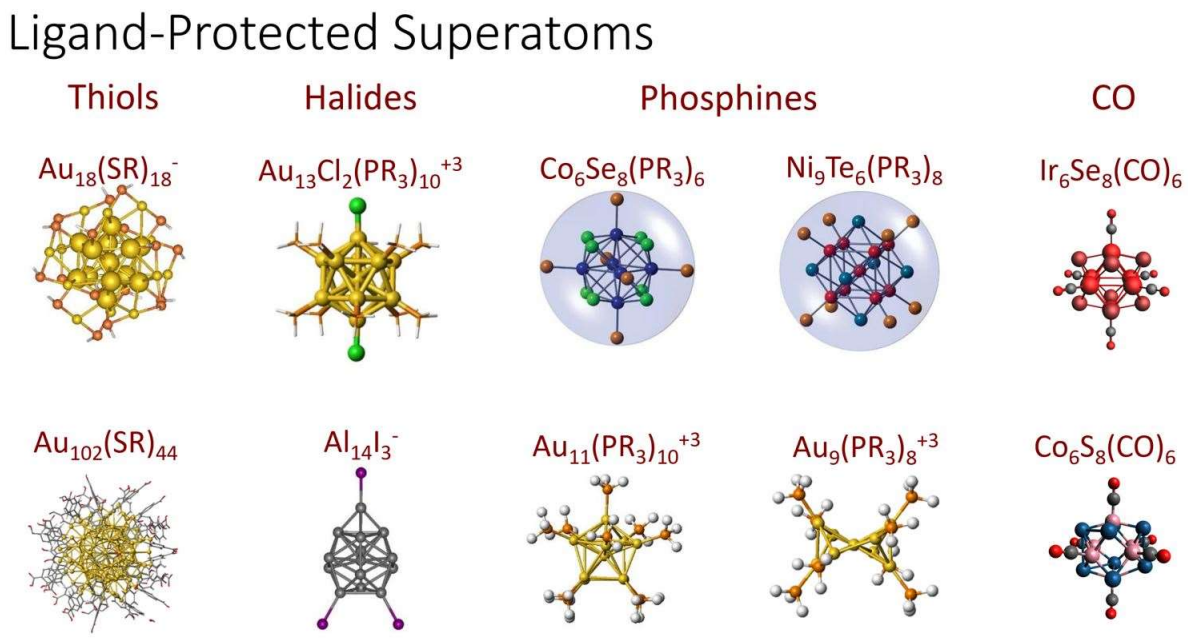

Figure 9: Examples of Ligand-Protected Superatoms

1.2 Motivation

The motivation for this work was founded on the fact that identifying the periodic properties in TMCC's is an outstanding problem in identifying organizational principles in clusters that are not noble or simple metal clusters. Specifically, we wanted to answer if there are periodic trends in TMCC. Since, the elements in the periodic table are arranged in order of increasing atomic number, unique characteristics of the periodic table can be determined. All of these elements display several other chemical, physical, and atomic trends that can be understood by using periodic law and table formation. The process of understanding these trends is done by analyzing the elements' electron configuration; a key aspect of the electron configuration is that all elements prefer a closed electronic shell, and will gain or lose electrons to form a preferred stable configuration. Studying the electronic configuration will supply knowledge that can be used to understand the periodic trends of clusters. Examples of periodic trends include Ionization Energy, Electron Affinity, Electronegativity, Metallic Character, Redox Potentials, etc. Periodic properties can have increased or decreased strength depending on the location of an atom on the periodic table. For example, a picture of the trend for electronegativity is seen in Figure 10. From Figure 10, we see that electronegativity increases up and to the right of the periodic table. Periodic property behavior has been observed in the nano electronic structure of clusters as seen in Figure 11. From Figure 11, we noticed that as the number of atoms within a cluster increases, periodic properties will vary in value. Additional periodic trend research regarding this problem will help answer an important problem for the field of cluster science and deepen our understanding of periodic properties.

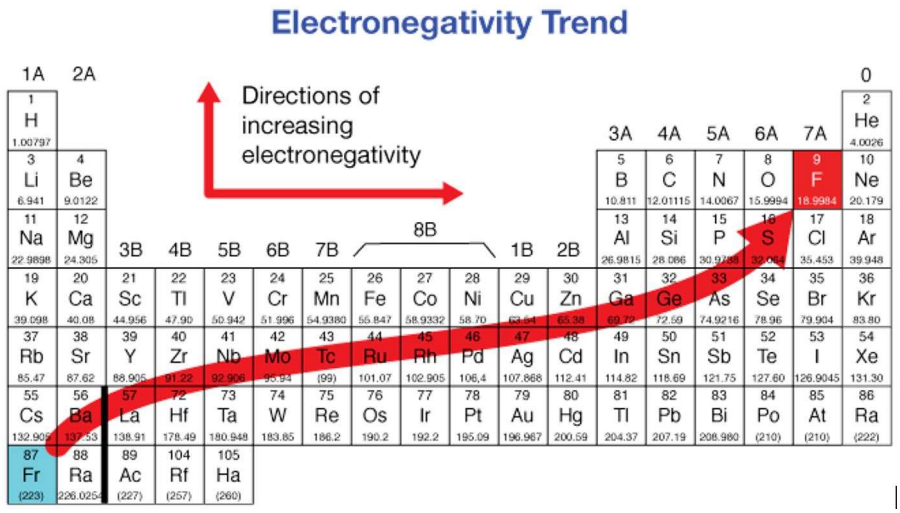

Figure 10: The trend of Electronegativity

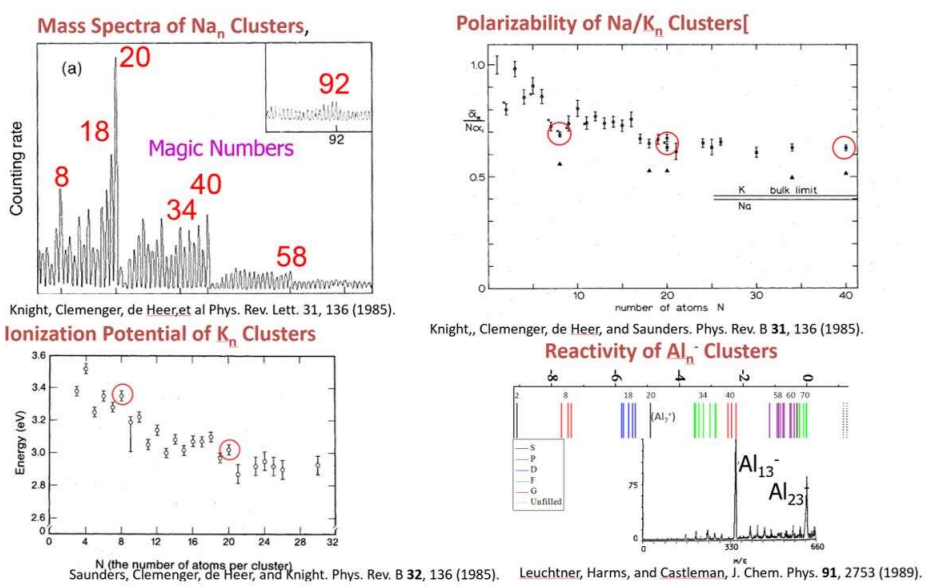

Figure 11: Trends in simple metal clusters that depend on valence electrons

As previously mentioned, superatoms represent an important topic in cluster science, and have enormous potential to construct materials with specially curated properties. This potential has sparked the synthesis of many types of clusters over the past few decades, with the creation of clusters containing many types of atoms and ligands investigated to catalogue the effects on stability and other attributes such as magnetism. For example, research by the Khanna Group has investigated the effects of ligands acting on the stability of metal chalcogenide clusters and the changes in the magnetic attributes [12]. The Khanna Group has also investigated the geometric effects ligands have on clusters [13]. Finally, A study performed by the Khanna Group on the Electronic structure of Cobalt Sulfide clusters demonstrated cluster properties are able to be fine-tuned to affect the charge density in regions [14]. Furthermore, the continued understanding of variables that affect the stability of different stable clusters has led to a better understanding of superatomic chemistry, which can enable the creation of new superatomic materials [15]. With many new developments on the horizon the development of cluster science is poised to generate exciting research.

II. Methods

2.1 DFT

As previously mentioned, the theoretical results presented in this paper are based on studies carried out using the Amsterdam Density Functional code to investigate how the infrared, optical, and molecular binding energy of Transition Metal Chalcogenide clusters changed as the number of valence electrons increased. The ADF program supports a wide variety of exchange–correlation (XC) functionals to determine charge densities. This means that if you know the charge density of a system, you can write a functional that converts charge density into an exchange correlation energy, which makes DFT extremely versatile. The exchange correlation function is written as:

$$E_{XC}[\rho] = (T[\rho] - T_s[\rho]) + (V_{ee}[\rho] - J[\rho])$$

ADF uses Density Functional Theory, which is one of the most notable and successful quantum-mechanical approaches in studying solid state physics and cluster systems.[16] Specifically, the theory can be used to calculate the electronic structure of many body systems by using functionals to determine the properties of systems, such as the binding energy of clusters and band structures. DFT can find the ground state of a system as large as 1000 valence electrons. This means that DFT can apply to biomolecules, crystals, and other systems in order to investigate the dynamics of those systems. Theoretical studies using DFT have provided data that has assisted in understanding complex biological processes at the molecular level. Depending upon the size of these systems, which can range from a few molecules to thousands of atoms, they can be studied by means of various quantum-chemical methods [17].

Two core theorems of DFT are the Hohenberg Kohn theorem and the Kohn-Sham equations. First published in 1964, the seminal paper by P. Hohenburg and W. Kohn was used to describe the ground state of an interacting electron gas in an external potential [18]. The Hohenberg-Kohn theorems describe any system where the electrons move under the influence of an external potential. Specifically, the Hohenberg Kohn theorem states that the ground state electron density of an electronic system is responsible for uniquely determining the external potential acting on the electrons up to an additive constant. The Kohn-Sham equations provide the computational scheme to calculate ground state electron density, and are given as:

$$\left[-\frac{1}{2}\nabla_i^2 + \hat{V}_{eff}(\vec{r}_i)\right]\psi_i = \epsilon_i\,\psi_i$$

Despite the popularity of DFT, there are still some calculations that the software has difficulty describing. These calculations can include van der Waals interactions, certain charge transfer excitations, transition states, global potential energy surfaces, dopant interactions, and some strongly correlated systems. There is robust discussion about the limitations of Ground State Density Functional Theory that has been presented in scientific literature. In general, for TMCC's we found that DFT accurately describes the electronic structure, and for this reason we are confident that DFT works reasonably well with TMCC [19].

2.2 ADF

Amsterdam Density Functional (ADF) is a program for first-principles electronic structure calculations that makes use of the aforementioned density functional theory (DFT). The Amsterdam Density Functional (ADF) program was developed in the early seventies and at that time was named HFS, for Hartree–Fock–Slater, with the explicit purpose to exploit the DFT computational advantages [20]. The ADF program incorporates relativistic effects with the ZORA formalism, in the scalar approach or with spin-orbit terms included. ADF uses Slater-type orbital functions to build Basis sets. Finally, energy gradients and second derivatives allow the computation of energy minima, transition states, reaction paths, and harmonic frequencies with IR intensities [20]. ADF has been used to calculate the electronic structure of many clusters, including Colloidal Au single-atom catalysts embedded on Pd nanoclusters [21]. Determining periodic properties in TMCC's required the collection of simulation data pertaining to numerous properties of TMCC. Consequently, ADF was used to investigate how the IR, OP, and molecular binding energy properties of 14 Transition Metal Chalcogenide clusters changed as the number of valence electrons increased. The 14 Transition Metal Chalcogenide clusters, in order of increasing valence electrons count, are as follows: $Ta_6Se_8(CO)_6$, $Ta_4W_2Se_8(CO)_6$, $Ta_2W_4Se_8(CO)_6$, $W_6Se_8(CO)_6$, $W_4Re_2Se_8(CO)_6$, $W_2Re_4Se_8(CO)_6$, $Re_6Se_8(CO)_6$, $Re_4Os_2Se_8(CO)_6$, $Re_2Os_4Se_8(CO)_6$, $Os_6Se_8(CO)_6$, $Os_4Ir_2Se_8(CO)_6$, $Os_2Ir_4Se_8(CO)_6$, $Ir_6Se_8(CO)_6$, $Ir_4Pt_2Se_8(CO)_6$. First, ADF was used to determine the converged coordinate systems of the clusters; this means that the SCF (Self-Consistent Field) has converged and the total energy of the system has been minimized. The self-consistent field (SCF) method is the standard algorithm for finding electronic structure configurations within Hartree-Fock and density functional theory. The self-consistent field method is an iterative method that involves selecting an approximate Hamiltonian, solving the Schrödinger equation to obtain a

more accurate set of orbitals, and then solving the Schrödinger equation again with these until the results converge. Self-consistent field (SCF), or mean-field methods, are widely used in physics to describe many-body problems. Because the SCF process is an iterative procedure, this meant that convergence issues could arise depending on numerous factors [22]. Next, we had to ensure that the atomic system under study used proper values of bond lengths, angles, and other internal degrees of freedom in the geometry. Finally, when copying the coordinates of atomic structures into the graphical user interface, we checked that the imported structure was complete and that no atoms were lost during the transition process. One advantage of using ADF is time dependent density functional theory (TD-DFT), which allows us to investigate the excitation energies and optical absorption of TMCC's. TD-DFT has previously been used to calculate the crystal structure, absorption band, and optical properties of Thiol protected Au_{25} cluster [23]. Additionally, the optical gap of $Au_{114}(SC_2H_4Ph)_{60}$ clusters was determined using TD-DFT [24]. Finally, TD-DFT has been utilized to study the origin of photoluminescence in nanoparticles [25]. We will summarize the results in the next section.

III. Results and Discussion

3.1 Structure of Clusters

We are interested in discovering if periodic behavior can be observed in octahedral metal-chalcogenide clusters**.** To accomplish this goal, we have carried out theoretical studies on octahedral metal-chalcogenide clusters using ADF. Prior literature studying octahedral metal-chalcogenide clusters has focused on multicentered bonding and quasi aromaticity [26]. Prior cluster structure research has included studying the Electronic Structures of Electron-Rich Octahedrally Condensed Transition-Metal Chalcogenide Clusters [27]. The final converged geometric structures were then visualized using the ADFView software program. A picture of all the converged geometries, with minimized total energy, is seen in Figure 12. In order to vary our clusters, we used electron counting. Electron counting can utilize different rules to determine the number of valence electrons in a cluster depending on the cluster elements and can be affected by the cluster geometry [28]. For example, the superatom complex electron counting rule was determined to be influenced by dopant atoms [29]. For our purposes, we have varied the transition metal to tune the valence count starting from 90 valence electrons. For example, for $Ta_6Se_8(CO)_6$, there are 5 valence electrons for the 6 Ta atoms (30 e^-), 6 valence electrons for the 8 Se atoms (48 e^-), and CO adds 2 valence electrons for the 6 CO molecules (12 e^-); so, $Ta_6Se_8(CO)_6$ has a total of 90 valence electrons and we successively replaced two transition metals with one that had a larger valence number so that we could go by two's up until 116 valence electrons. We noticed 96 to 100 and 114 valence electrons resulted in increased stability.

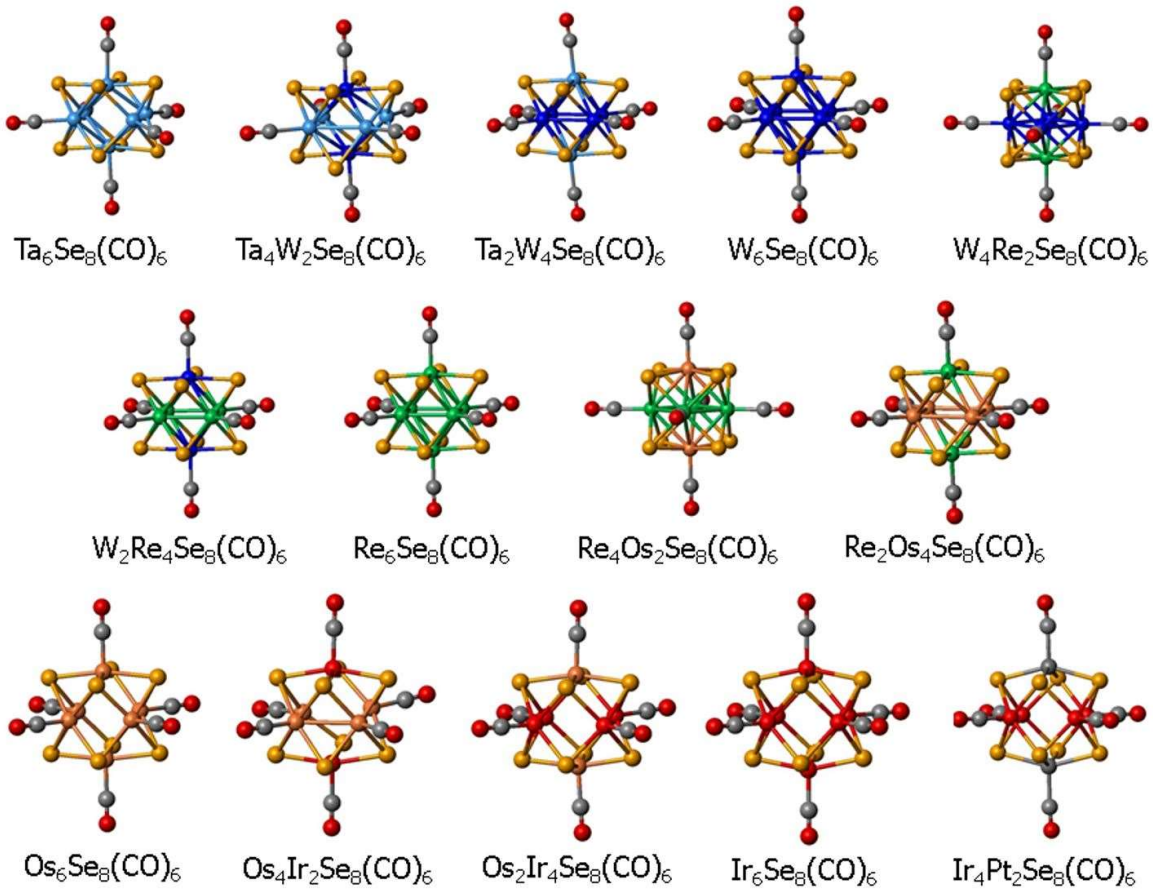

Figure 12: A picture of the converged geometric coordinates for the 14 Metal Chalcogenide Clusters studied in the research

3.2 Optical Spectroscopy in TMCC's

The optical spectroscopy behavior of TMCC's is important because prior research has shown a connection between charge transfer of molecular clusters and the absorption intensity of the optical spectroscopy; data about this relationship will be useful for analyzing the energetics behavior of TMCC's [30]. To investigate properties of the optical spectra, we calculated the optical absorption spectra of TMCC's from a valence electron counts of 90 to 116, with a variation of successive valence electrons. The lowest excitation state was determined using TD-DFT. The Lowest Excitation State (LES) is defined as the lowest possible excited energy level of the cluster. We confirmed during our research that the LES noticeably changed as the number of valence electrons increased, which was a periodic trend that changed as the number of valence electrons increased. A graph of lowest excitation state as a function of valence electrons is seen in Figure 13. We noticed large peaks in the Lowest Excitation State at 96, 100, and 114 valence electrons. This is evidence of electronic shell closure and a large gap between occupied and unoccupied levels, and was evidence that 96, 100, and 114 were magic numbers. To further investigate the periodic properties of the optical frequency, the optical absorption intensity of the individual clusters was determined using ADF. First, we confirmed during our research that the absorption intensity noticeably changed as the number of valence electrons increased. A graph of optical absorption intensity as a function of valence electrons is seen in Figure 14 for the selected clusters. The clusters: $W_6Se_8(CO)_6$, $W_2Re_4Se_8(CO)_6$, $Os_6Se_8(CO)_6$, and $Ir_6Se_8(CO)_6$ were chosen to represent a large spread of valence electron numbers, with 108 being an example of a cluster with an observable gap. This in turn would allow us to determine general changes in the behavior of trends. In the next section, we discuss the energetics of select clusters.

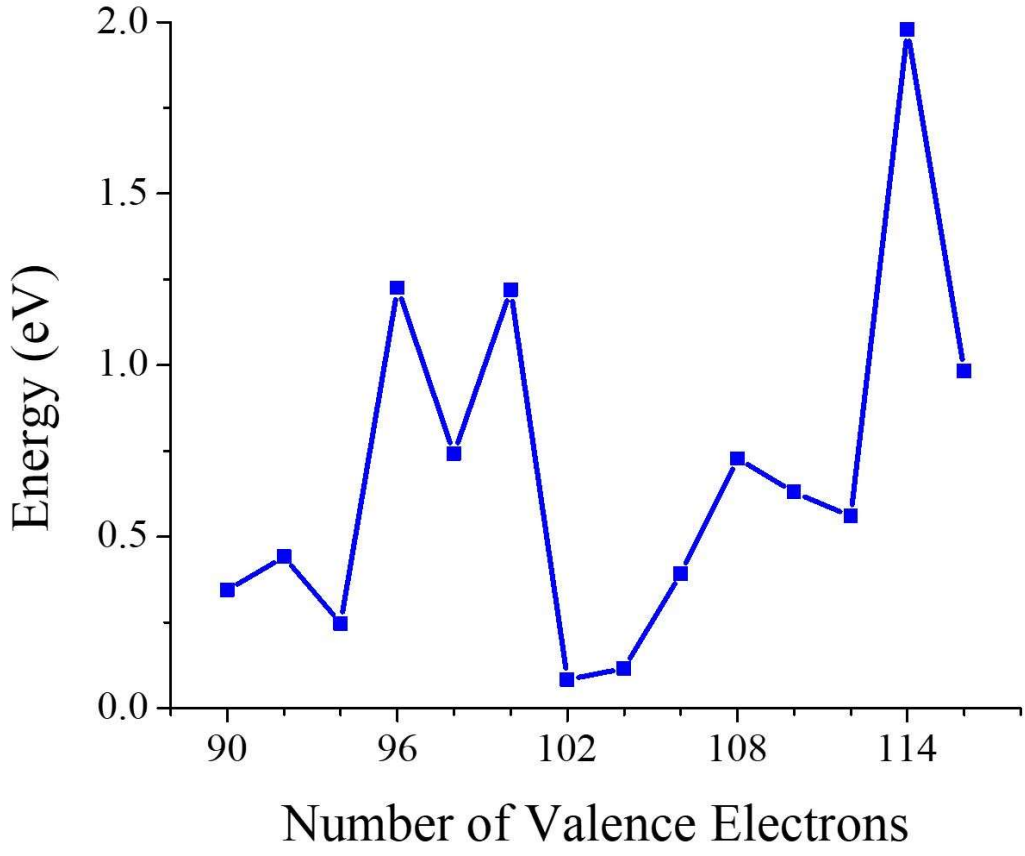

Figure 13: A picture of the lowest excitation state vs valence electrons

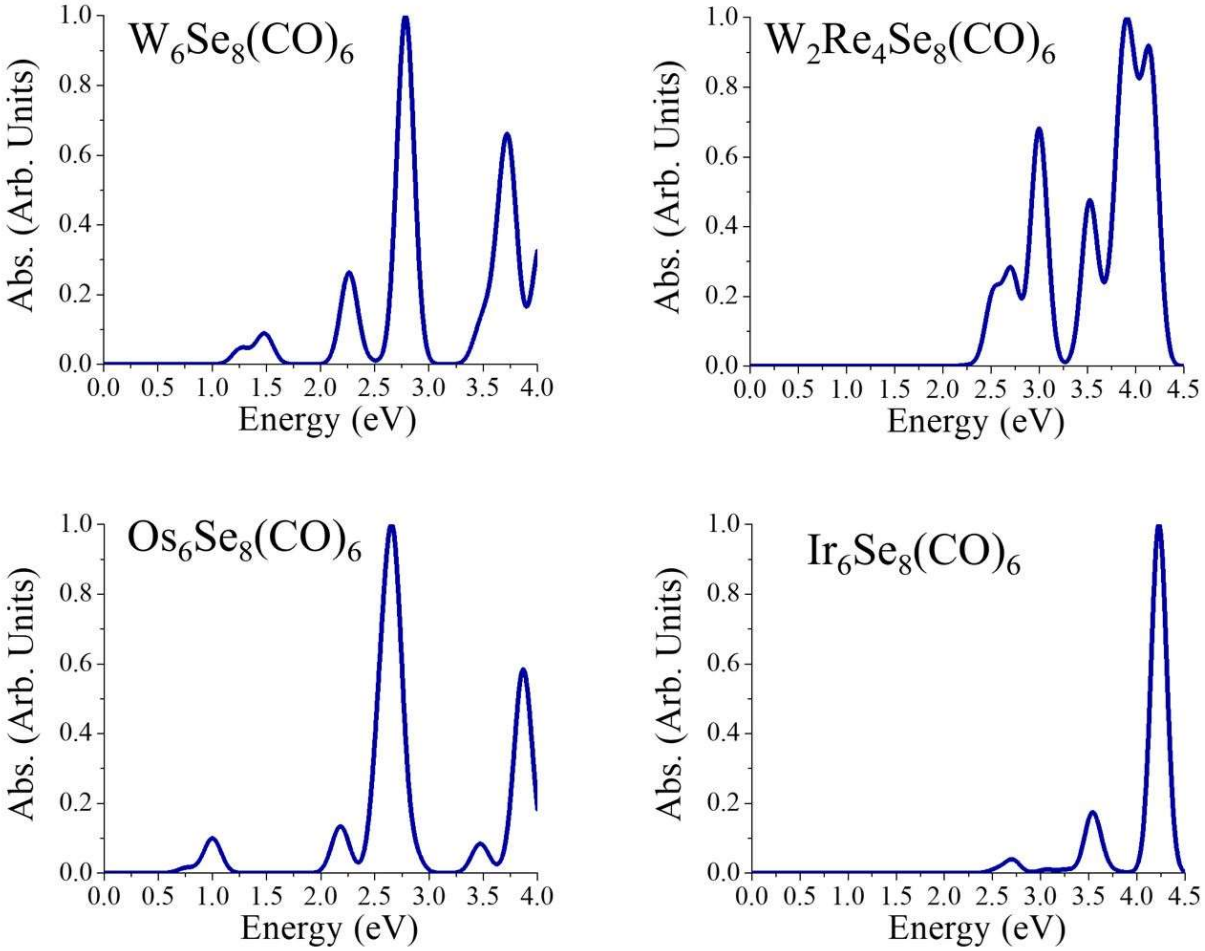

Figure 14: A graph of optical absorbance as a function of the photon energy for $W_6Se_8(CO)_6$, $W_2Re_4Se_8(CO)_6$, $Os_6Se_8(CO)_6$, $Ir_6Se_8(CO)_6$. Which corresponds to 96, 100, 108 and 114 valence electrons respectively.

3.3 Energetics Results

The graphs in Figure 15 communicate energetics periodic trends that are seen in the infrared of clusters as the number of valence electrons increased. For example, the Atomization Energy starts to steadily decrease after 96 valence electrons, with two large drop offs in atomization energy at 102 and 116. This implies enhanced stability after 96 valence electrons. Using $Ta_6Se_8(CO)_6$ as an example, we define the atomization energy as:

$$\Delta E\ (eV) = 6(Ta) + 8(Se) + 6(CO) - Ta_6Se_8(CO)_6$$

The CO Binding Energy steadily increased as the number of valence electrons increased, with a reversal in behavior after 114 valence electrons. Using $Ta_6Se_8(CO)_6$ as an example, we define the CO Binding Energy as:

$$\Delta E(eV) = Ta_6Se_8(CO)_5 + CO - Ta_6Se_8(CO)_6$$

The Total CO Binding Energy steadily increased as the number of valence electrons increased, with a notable drop off at 102 and 114 valence electrons. Using $Ta_6Se_8(CO)_6$ as an example, we define the Total CO Binding Energy as:

$$\Delta E\ (eV) = Ta_6Se_8 + 6(CO) - Ta_6Se_8(CO)_6$$

Finally, the Hirschfeld Charge CO increased steadily up to 100 valence electrons before a series of large drop offs, and then increased until peaking at 114 valence electrons. We determined the reason for the behavior in the Hirschfeld Charge graph is due to back-bonding, which means the charges transfer to the CO. The fact that there is little charge transfer for W_2Re_4 in the closed electron shell, is likely due to reduced back-bonding. If the CO is more positive, there is reduced back-bonding; if the CO is negative, there is more back-bonding.

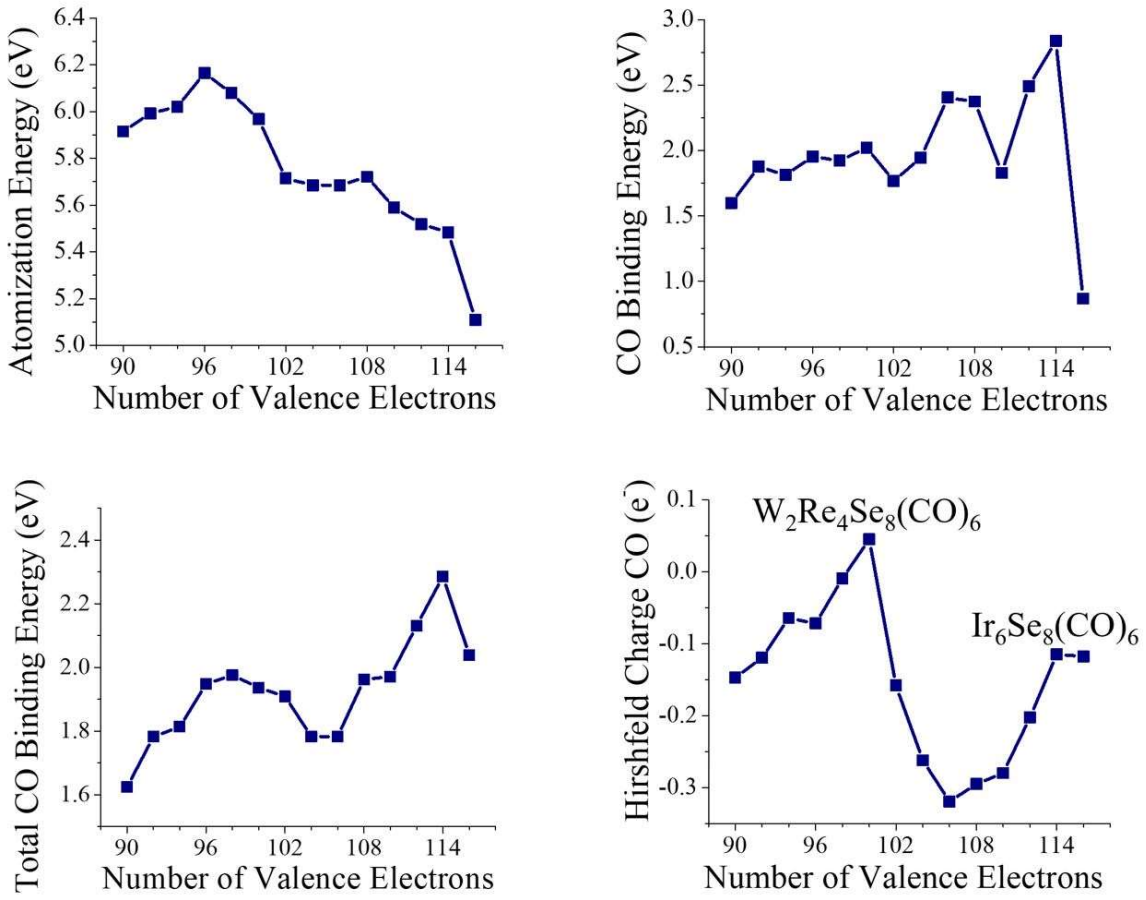

Figure 15: The atomization energy, CO binding energy, total CO binding energy, and Hirshfeld charge on the CO molecules for the $TM_6Se_8(CO)_6$ clusters.

3.4 Infrared Frequency Results

To investigate properties of the infrared frequency, we calculated the infrared frequency of TMCC from a valence electron counts of 90 to 116, with a variation of successive valence electrons. For the IR spectra analysis, four primary clusters were chosen to demonstrate the relation between IR absorption intensity and energy. These four clusters were chosen due to the range of valence electrons that are represented, which allowed us to determine general conclusions about the IR behavior of these clusters. A graph of these four clusters is presented in Figure 16. The graphs communicate that the lower energy absorption peaks are noticeably affected by a change in the number of valence electrons compared to the absorption intensity at higher energy levels. For example, the $Ir_6Se_8(CO)_6$ cluster, which has the largest valence electron number, demonstrated absorption intensity peaks almost exclusively around the 500cm^{-1} range. Next, we made a graph of CO Absorption as a function of valence electrons, which can be seen in Figure 17. From the results of Figure 17, we determined that the charge transfer and CO bond noticeably depend on one another, which can be seen in Figure 18. The two graphs in Figure 18 demonstrated almost the exact same behavior. To further investigate this behavior, we analyzed the metal carbon asymmetric stretch to determine the relationship to the number of valence electrons, which can be seen in Figure 19. We noticed that as the number of valence electrons increased so did the M-C Asymmetric Stretch. Figure 19 displays two steep increases in the M-C stretch length at 94 and 98 valence electrons. A general trend of the M-C bond length is given in Figure 20. From Figure 20, we see that the two separate lines correspond to a smaller Z as the starting element in a cluster or the larger Z to graph distinctive behavior of the M-C bond length as a function of the number of valence electrons. From Figure 20, we noticed that as the number of valence electrons increased for larger z the M-C Bond Length decreases faster compared to smaller Z. This behavior is

consistent until 116 valence electrons, when the behavior reverses as the MC- Bond Length sharply increased for larger z value. From prior literature, we know that the metal carbon bond length is an important variable that can influence catalysis [31]. The M-C Asymmetric stretch will be further evaluated in the Infrared Frequency Results section.

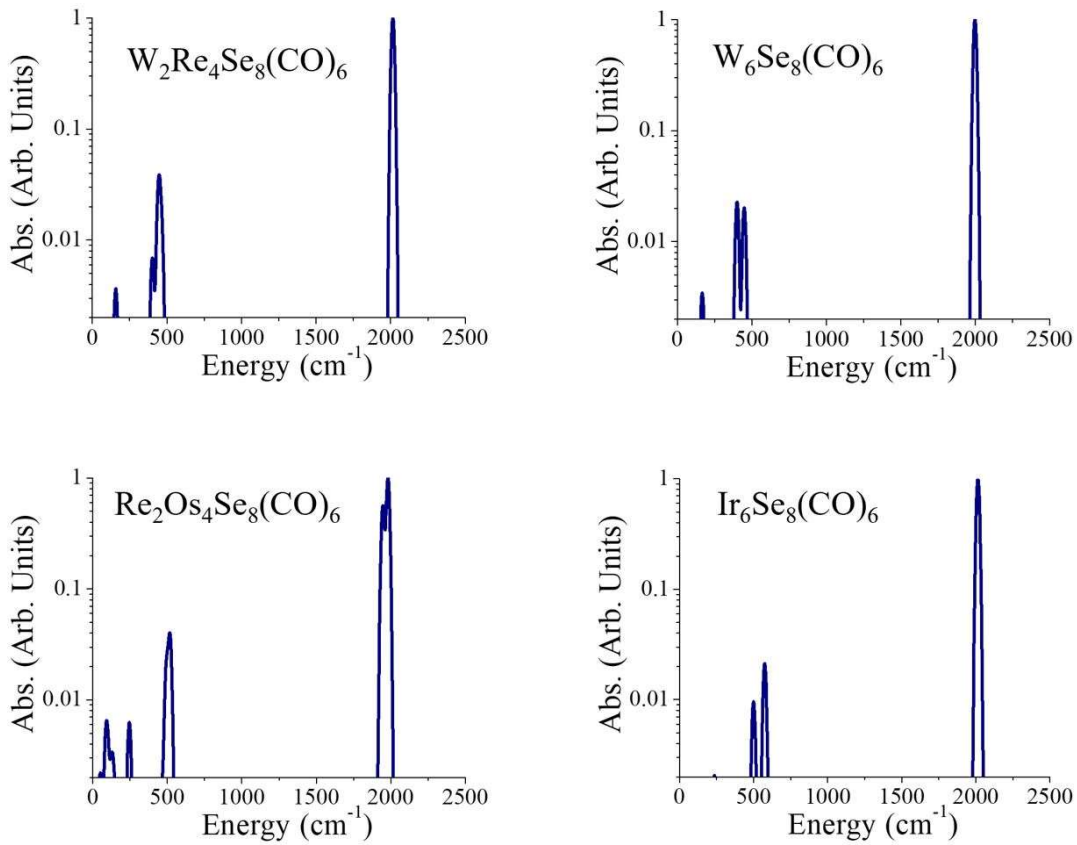

Figure 16: The IR Intensity vs Valence Electrons for selected clusters

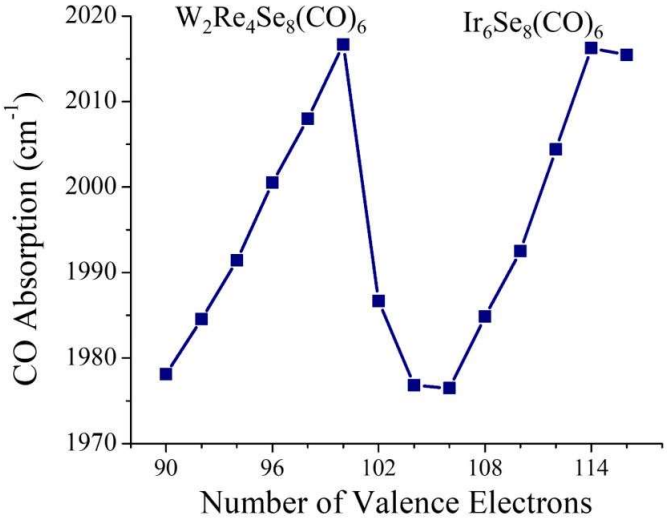

Figure 17: CO Absorption energy vs Number of Valence Electrons

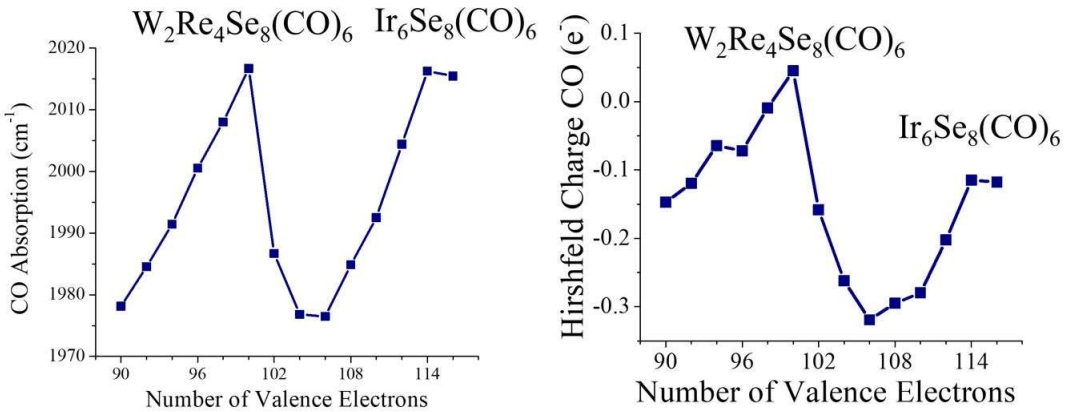

Figure 18: CO Absorption energy and Hirshfeld Charge CO(e^-) comparison

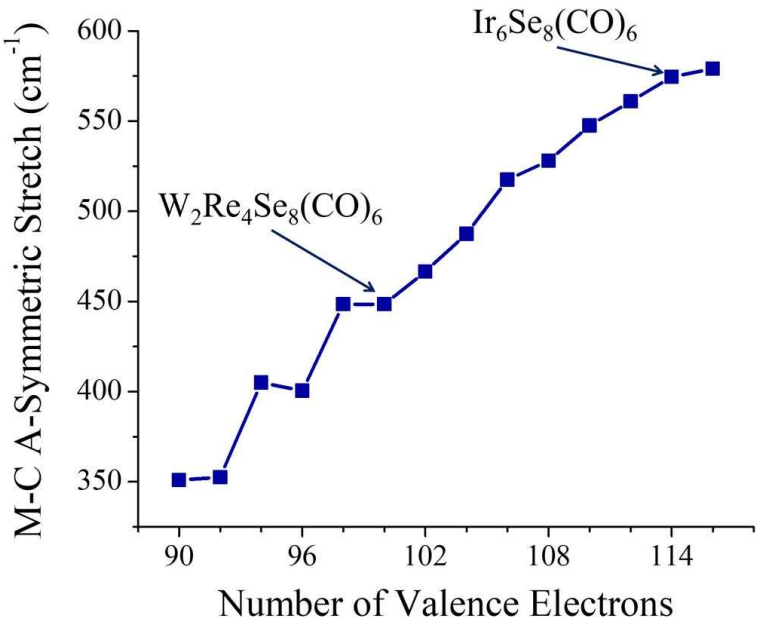

Figure 19: MC-Antisymmetric stretch energy in cm-1 as a function of the valence electron count.

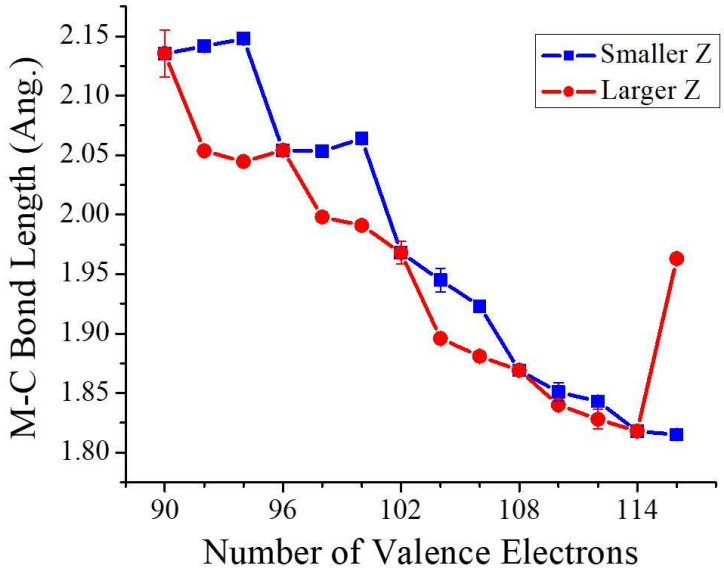

Figure 20: Metal Carbon bond length for smaller Z and larger Z

Graphs of the individual IR behavior for the Ta family of clusters are presented in Figures 21, 22, and 23. The numerous individual graphs created to display absorption intensity vs energy for all 14 MCC were combined to create a composite IR absorption graph. The combined IR absorption graph as a function of energy can be seen in Figure 24. In Figure 24, we noticed that the energy of the absorption peak shifted to the right as the number of valence electrons increased. Furthermore, as the number of valence electrons increased the absorption intensity peaks decreased, this is most prevalent towards the far right. To determine why that happened, we investigated the Normal Modes of the clusters in order to determine the direction of displacement for the atoms.

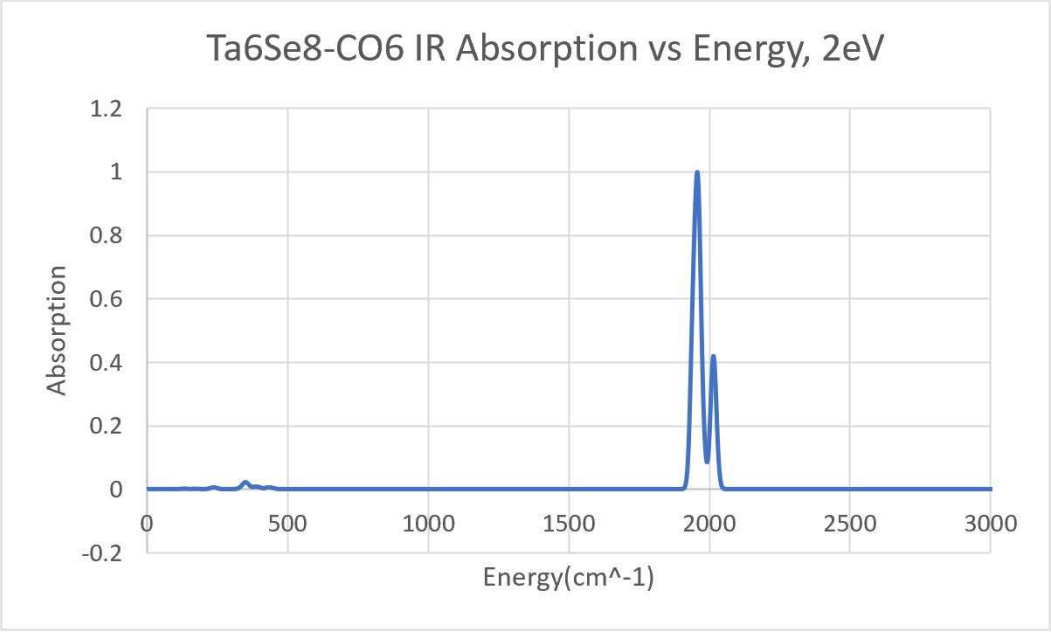

Figure 21: The IR Intensity vs Valence Electrons for $Ta_6Se_8(CO)_6$ clusters

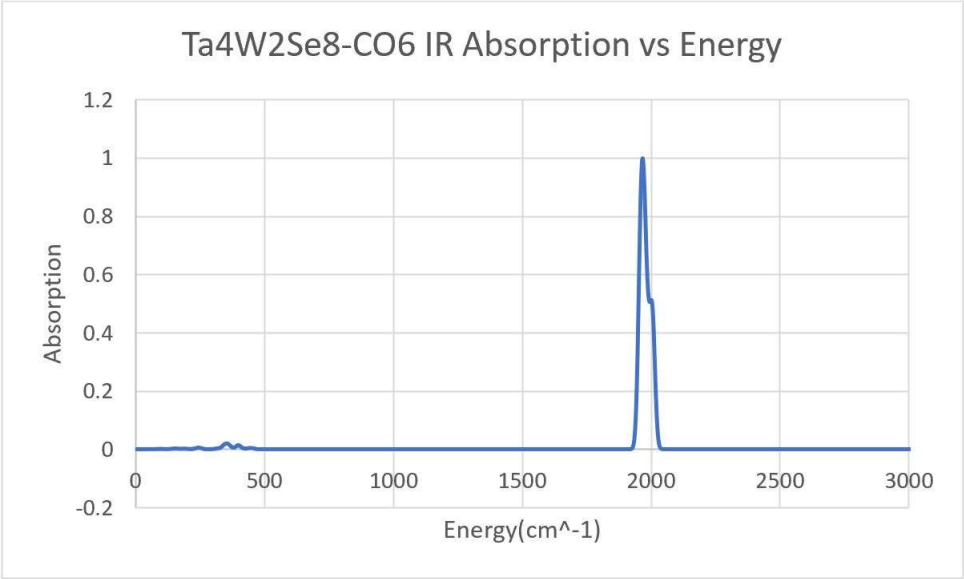

Figure 22: The IR Intensity vs Valence Electrons for $Ta_4W2Se8(CO)_6$ clusters

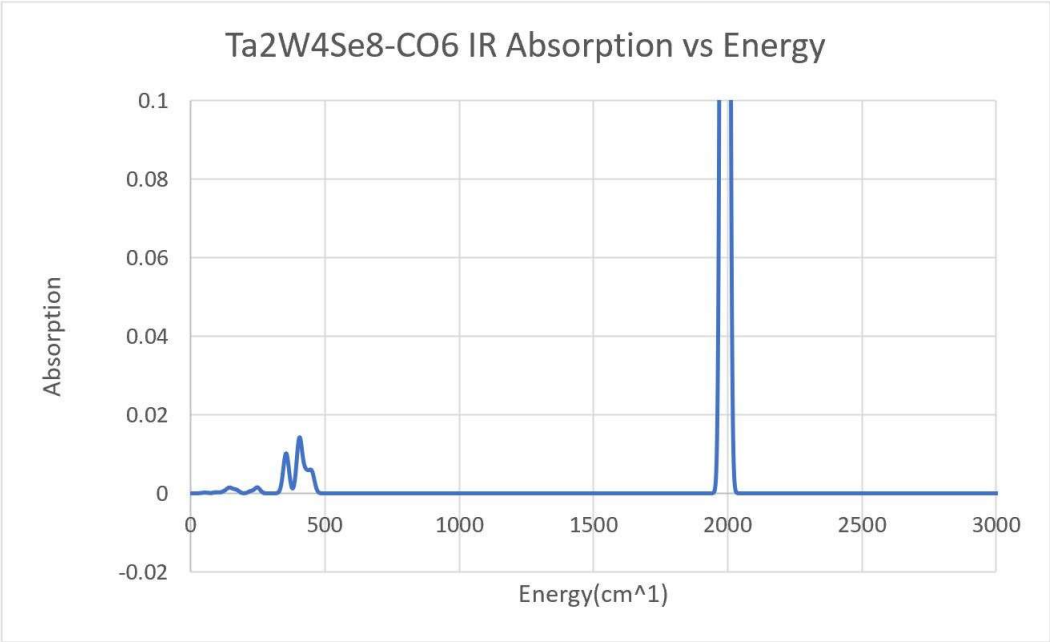

Figure 23: The IR Intensity vs Valence Electrons for $Ta_4W2Se8(CO)_6$ clusters

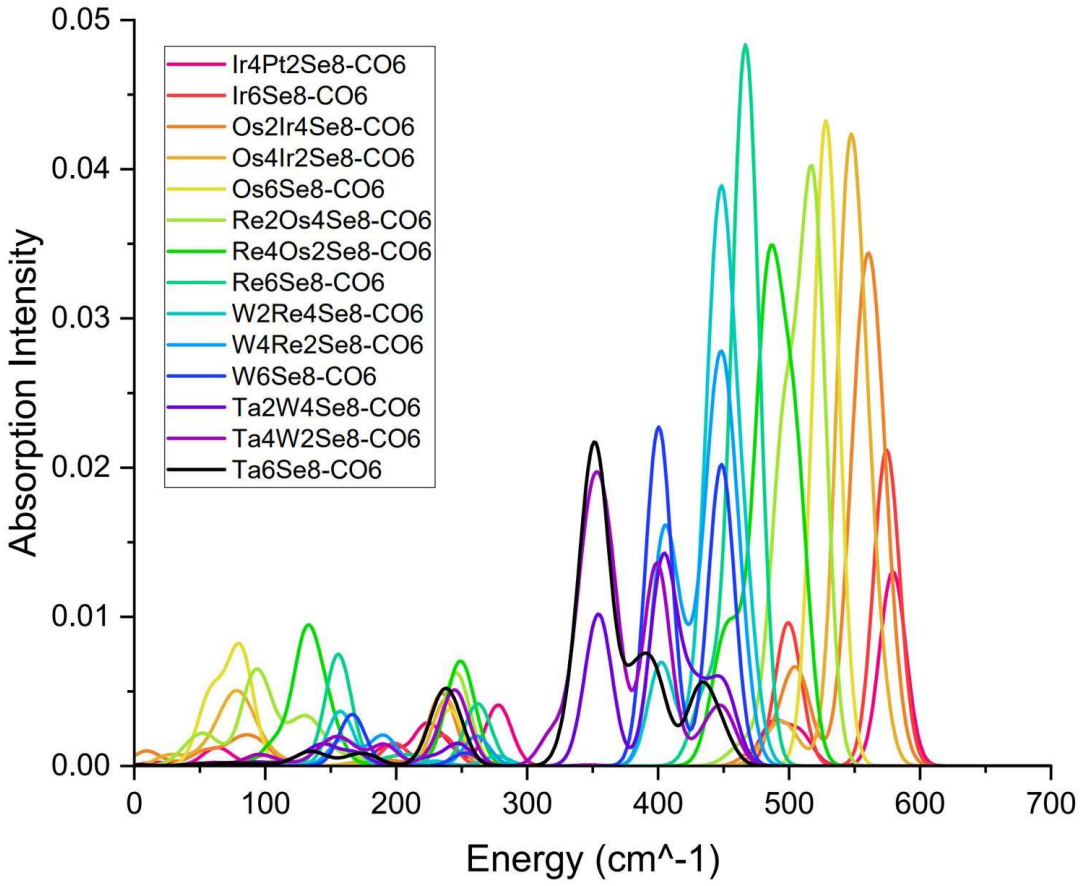

Figure 24: The Composite IR absorption intensity vs energy graph

The normal modes of an oscillating system are patterns of motion in which all parts of the system move sinusoidally with the same frequency and with a fixed phase relation. A picture of the normal modes of each cluster, with visible displacement vectors, are seen in Figure 25, with the energy of the normal modes listed at the bottom of each cluster. For the four visible clusters, we noticed that $W_5Se_8(CO)_6$, $Re_2Os_4Se_8(CO)_6$, and $Ir_6Se_8(CO)_6$ all have asymmetric displacements, while $W_2Re_4Se_8(CO)_6$ has a waggle displacement. In all examples, the asymmetric displacement is along the CO molecules. We noticed that all of the strongest displacements were among antisymmetric stretches, this is because they were optically active with a dipole. This fact is important to note since the existence of dipoles are critical to potential chemical control applications [32]. The second highest set of absorptions are the metal carbon stretches, and this is to be expected because low mass in the CO equates to a higher energy excitation.

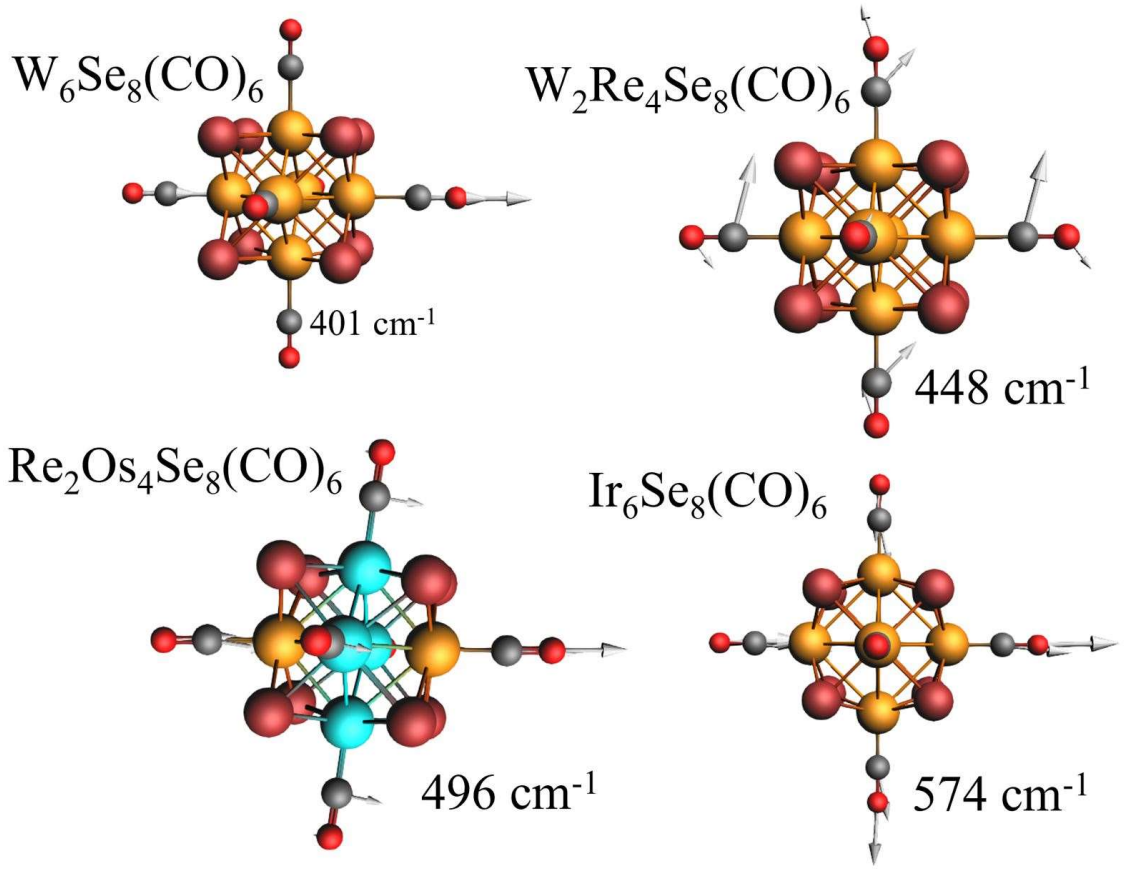

Figure 25: The Cluster Normal Modes with visible displacement vectors

IV. Conclusions

Prior work has studied the effects of ligands and valence electrons on the electronic properties and electrical transport in clusters [33]. This study contributes to the collection of prior work by further studying the periodic properties of clusters in order to understand their influence on the properties of clusters. During the course of our investigation, we determined the existence of several periodic trends in octahedral Transition Metal Chalcogenide Clusters $TM_6Se_8(CO)_6$. In order to investigate further, the ground state, optical spectra, and infrared spectra of doped transition metal chalcogenide clusters with 90-116 valence electrons were calculated. The number of valence electrons were increased from Ta6Se8 by adding, or doping, two of the transition metals with an atomic number that is one higher until it is fully doped. The electron counting was done by counting all the valence electrons of the transition metal and selenium and we added two valence electrons for every carbon monoxide molecule. We found that octahedral metal-chalcogenide clusters with 96, 100, and 114 have larger excitation energies, which is consistent with these clusters having closed-electronic shells. Periodic trends were also observed in the Infrared spectra, with the CO bond stretch having the highest energy at 100 valence electrons, and a significant peak at 114 valence electrons due to the closed-electronic shell minimizing back-bonding with the CO molecule. The origin of this can be seen in the Hirshfeld charge, where there is reduced back-bonding when the cluster has a closed electronic shell. Back-bonding causes a decrease in the CO stretch energy; thus, reducing back-bonding causes a stretch. A periodic trend in the antisymmetric TM-C stretch was also observed, with the vibrational energy increasing as the valence electron count increased. This is due to decrease in the TM-C bond length resulting in a larger force constant. These results reveal that periodic trends can be found in clusters other than simple or noble metal clusters, they can also be observed in symmetric transition-metal chalcogenide

clusters. Further, these trends can be observed via optical and infrared spectroscopy showing that the superatom concept in metal chalcogenide clusters goes beyond electronic excitations, and can be seen in other observable properties.

V. Bibliography

[1] *Materials and Man's Needs: Materials Science and Engineering* (Washington, DC: The National Academies Press, 1974), https://doi.org/10.17226/10435.

[2] Shiv N. Khanna et al., "The Superatomic State beyond Conventional Magic Numbers: Ligated Metal Chalcogenide Superatoms," *The Journal of Chemical Physics* 155, no. 12 (September 28, 2021): 120901, https://doi.org/10.1063/5.0062582; Arthur C. Reber and Shiv N. Khanna, "Superatoms: Electronic and Geometric Effects on Reactivity," *Accounts of Chemical Research* 50, no. 2 (February 21, 2017): 255–63, https://doi.org/10.1021/acs.accounts.6b00464; A. W. Castleman and S. N. Khanna, "Clusters, Superatoms, and Building Blocks of New Materials†," *J. Phys. Chem. C* 113, no. 7 (2009): 2664–75, https://doi.org/10.1021/jp806850h.

[3] Arthur C. Reber et al., "Superatomic Molecules with Internal Electric Fields for Light Harvesting," *Nanoscale* 12, no. 7 (2020): 4736–42, https://doi.org/10.1039/C9NR09229C; Dinesh Bista et al., "A Ligand-Induced Homojunction between Aluminum-Based Superatomic Clusters," *Nanoscale* 12, no. 22 (June 11, 2020): 12046–56, https://doi.org/10.1039/D0NR02611E.

[4] Xavier Roy et al., "Nanoscale Atoms in Solid-State Chemistry," *Science* 341, no. 6142 (July 12, 2013): 157–60, https://doi.org/10.1126/science.1236259; Evan A. Doud et al., "Superatoms in Materials Science," *Nature Reviews Materials* 5, no. 5 (May 2020): 371–87, https://doi.org/10.1038/s41578-019-0175-3.

[5] Vikas Chauhan, Arthur C. Reber, and Shiv N. Khanna, "Metal Chalcogenide Clusters with Closed Electronic Shells and the Electronic Properties of Alkalis and Halogens," *Journal of the American Chemical Society* 139, no. 5 (February 8, 2017): 1871–77, https://doi.org/10.1021/jacs.6b09416.

[6] Arthur C. Reber and Shiv N. Khanna, "The Effect of Chalcogen and Metal on the Electronic Properties and Stability of Metal–Chalcogenides Clusters, TM6Xn(PH3)6 (TM = Mo, Cr, Re, Co, Ni; X = Se, Te; n = 8,5)," *The European Physical Journal D* 72, no. 11 (November 1, 2018): 199, https://doi.org/10.1140/epjd/e2018-90223-7.

[7] Shoushou He et al., "Site-Selective Surface Modification of 2D Superatomic Re6Se8," *Journal of the American Chemical Society* 144, no. 1 (January 12, 2022): 74–79, https://doi.org/10.1021/jacs.1c10833.

[8] Amymarie K. Bartholomew et al., "Superatom Regiochemistry Dictates the Assembly and Surface Reactivity of a Two-Dimensional Material," *Journal of the American Chemical Society* 144, no. 3 (January 26, 2022): 1119–24, https://doi.org/10.1021/jacs.1c12072.

[9] Dinesh Bista et al., "High-Spin Superatom Stabilized by Dual Subshell Filling," *Journal of the American Chemical Society* 144, no. 11 (March 23, 2022): 5172–79, https://doi.org/10.1021/jacs.2c00731.

[10] Weijie Zhao et al., "Evolution of Electronic Structure in Atomically Thin Sheets of WS2 and WSe2," *ACS Nano* 7, no. 1 (January 22, 2013): 791–97, https://doi.org/10.1021/nn305275h.

[11] D. E. Bergeron et al., "Al Cluster Superatoms as Halogens in Polyhalides and as Alkaline Earths in Iodide Salts," *Science* 307, no. 5707 (January 14, 2005): 231–35, https://doi.org/10.1126/science.1105820.

[12] Vikas Chauhan, Arthur C. Reber, and Shiv N. Khanna, "CO Ligands Stabilize Metal Chalcogenide Co 6 Se 8 (CO) n Clusters via Demagnetization," *Physical Chemistry Chemical Physics* 19 (2017): 31940, https://doi.org/10.1039/C7CP07606A.

[13] Rajini Anumula et al., "Ligand Accommodation Causes the Anti-Centrosymmetric Structure of Au 13 Cu 4 Clusters with near-Infrared Emission," *Nanoscale* 12, no. 27 (2020): 14801–7, https://doi.org/10.1039/D0NR02448A.

[14] Gaoxiang Liu et al., "Ligand Effect on the Electronic Structure of Cobalt Sulfide Clusters: A Combined Experimental and Theoretical Study," *The Journal of Physical Chemistry C* 123, no. 41 (October 17, 2019): 25121–27, https://doi.org/10.1021/acs.jpcc.9b04153.

[15] Jaeeun Yu et al., "Patterning Superatom Dopants on Transition Metal Dichalcogenides," *Nano Letters* 16, no. 5 (May 11, 2016): 3385–89, https://doi.org/10.1021/acs.nanolett.6b01152.

[16] Klaus Capelle, "A Bird's-Eye View of Density-Functional Theory," *ArXiv:Cond-Mat/0211443*, November 20, 2002, http://arxiv.org/abs/cond-mat/0211443.

[17] Tomasz Adam Wesolowski and Jacques Weber, "Applications of Density Functional Theory to Biological Systems," in *Applications of Density Functional Theory to Biological Systems* (Oxford University Press, 1998), https://doi.org/10.1093/oso/9780195098730.003.0009.

[18] P. Hohenberg and W. Kohn, "Inhomogeneous Electron Gas," *Physical Review* 136, no. 3B (November 9, 1964): B864–71, https://doi.org/10.1103/PhysRev.136.B864.

[19] John P. Perdew et al., "Some Fundamental Issues in Ground-State Density Functional Theory: A Guide for the Perplexed," *Journal of Chemical Theory and Computation* 5, no. 4 (April 14, 2009): 902–8, https://doi.org/10.1021/ct800531s.

[20] G. te Velde et al., "Chemistry with ADF," *Journal of Computational Chemistry* 22, no. 9 (July 15, 2001): 931–67, https://doi.org/10.1002/jcc.1056.

[21] Haijun Zhang et al., "Colloidal Au Single-Atom Catalysts Embedded on Pd Nanoclusters," *Journal of Materials Chemistry A* 2, no. 33 (July 29, 2014): 13498–508, https://doi.org/10.1039/C4TA01696C.

[22] "SCF Convergence Guidelines for ADF — ADF 2022.1 Documentation," accessed March 22, 2022, https://www.scm.com/doc/ADF/Rec_problems_questions/SCF.html.

[23] Manzhou Zhu et al., "Correlating the Crystal Structure of A Thiol-Protected Au25 Cluster and Optical Properties," *J. Am. Chem. Soc.* 130, no. 18 (2008): 5883–85, https://doi.org/10.1021/ja801173r.

[24] Jaakko Koivisto et al., "Experimental and Theoretical Determination of the Optical Gap of the Au144(SC2H4Ph)60 Cluster and the (Au/Ag)144(SC2H4Ph)60 Nanoalloys," *The Journal of Physical Chemistry Letters* 3, no. 20 (October 18, 2012): 3076–80, https://doi.org/10.1021/jz301261x.

[25] K. L. Dimuthu M. Weerawardene and Christine M. Aikens, "Origin of Photoluminescence of Ag25(SR)18– Nanoparticles: Ligand and Doping Effect," *The Journal of Physical Chemistry C* 122, no. 4 (February 1, 2018): 2440–47, https://doi.org/10.1021/acs.jpcc.7b11706.

[26] Zhida Chen, "Multicentered Bonding and Quasi-Aromaticity in Metal-Chalcogenide Cluster Chemistry," *Journal of Cluster Science* 6, no. 3 (September 1, 1995): 357–77, https://doi.org/10.1007/BF01165467.

[27] Régis Gautier et al., "Electronic Structures of Electron-Rich Octahedrally Condensed Transition-Metal Chalcogenide Clusters," *Inorganic Chemistry* 41, no. 4 (February 1, 2002): 796–804, https://doi.org/10.1021/ic010812b.

[28] J. Ulises Reveles and S. N. Khanna, "Electronic Counting Rules for the Stability of Metal-Silicon Clusters," *Physical Review B* 74, no. 3 (July 28, 2006): 035435, https://doi.org/10.1103/PhysRevB.74.035435.

[29] P. Andre Clayborne et al., "Evidence of Superatom Electronic Shells in Ligand-Stabilized Aluminum Clusters," *The Journal of Chemical Physics* 135, no. 9 (September 6, 2011): 094701, https://doi.org/doi:10.1063/1.3632087.

[30] Jessica L. Shott et al., "Ball and Socket Assembly of Binary Superatomic Solids Containing Trinuclear Nickel Cluster Cations and Fulleride Anions," *Inorganic Chemistry* 56, no. 18 (September 18, 2017): 10984–90, https://doi.org/10.1021/acs.inorgchem.7b01259.

[31] J. A. Martinho Simoes and J. L. Beauchamp, "Transition Metal-Hydrogen and Metal-Carbon Bond Strengths: The Keys to Catalysis," *Chemical Reviews* 90, no. 4 (June 1, 1990): 629–88, https://doi.org/10.1021/cr00102a004.

[32] Dinesh Bista, Turbasu Sengupta, and Shiv N. Khanna, "Massive Dipoles across the Metal–Semiconductor Cluster Interface: Towards Chemically Controlled Rectification," *Physical Chemistry Chemical Physics* 23, no. 34 (September 1, 2021): 18975–82, https://doi.org/10.1039/D1CP02420E.

[33] Hennrik Schmidt, Francesco Giustiniano, and Goki Eda, "Electronic Transport Properties of Transition Metal Dichalcogenide Field-Effect Devices: Surface and Interface Effects," *Chemical Society Reviews* 44, no. 21 (October 19, 2015): 7715–36, https://doi.org/10.1039/C5CS00275C; Albert Armstrong et al., "Al Valence Controls the Coordination and Stability of Cationic Aluminum–Oxygen Clusters in Reactions of Aln+ with Oxygen," *The Journal of Physical Chemistry A* 123, no. 34 (August 29, 2019): 7463–69, https://doi.org/10.1021/acs.jpca.9b05646; Albert Armstrong, Arthur C. Reber, and Shiv N. Khanna, "Multiple-Valence Aluminum and the Electronic and Geometric Structure of AlnOm Clusters," *The Journal of Physical Chemistry A* 123, no. 24 (June 20, 2019), https://doi.org/10.1021/acs.jpca.9b01729.